Dynamic Light-Scattering Studies of Poly(γ-benzyl α, l-glutamate)–Benzyl Alcohol System

PREMAL SHUKLA,[1] M. MUTHUKUMAR,[1,*] and KENNETH H. LANGLEY[2]

[1]Departments of Polymer Science & Engineering and [2]Department of Physics and Astronomy, University of Massachusetts, Amherst, MA 01003

SYNOPSIS

We report the concentration and temperature dependencies of the diffusion coefficients obtained from dynamic light-scattering studies for the poly(γ-benzyl α, l-glutamate)-benzyl alcohol (PBLG–BA) system. These studies were made at dilute and semidilute polymer concentrations, mainly in the isotropic phase. The measured translational and rotational diffusion coefficients in dilute solutions are consistent with predictions based on wormlike chain models. The mutual diffusion coefficient in semidilute solutions shows a marked deviation from scaling predictions, demonstrating the strong coupling between the translational and rotational motions. The measured time evolution of the scattered intensity after the PBLG–BA system is suddenly quenched into the gel phase demonstrates that aggregation is a significant mechanism in the formation of the gel phase.

INTRODUCTION

The problem of ordering rigid rods in solution was first considered by Onsager.[1] His analysis was valid for low concentrations and was based on the second virial coefficient. He showed that a solution of rodlike particles with hard interactions undergoes a thermodynamic phase transition as the particle concentration is increased. Flory[2] presented a lattice theory of solutions of semiflexible polymer chains and predicted a phase diagram consisting of three distinct phases depending upon the temperature and polymer concentration. At sufficiently low polymer concentrations and high temperature, the solution is in the isotropic phase. Between the concentrations, referred to as the Robinson A and Robinson B points,[3,4] and at high temperatures, the solution is the narrow biphasic phase, wherein the isotropic and liquid crystalline phases coexist. Beyond the concentration corresponding to the Robinson B point and at high temperatures, the solution is in the liquid crystalline phase. At lower temperatures, all regions go into the wide biphasic phase, where, again, the isotropic and liquid crystalline phases are supposed to coexist. The Flory phase diagram is shown schematically in Figure 1.

There have been extensive experimental studies reported in the literature over the past several decades regarding the phase diagram and properties of polymer solutions in different phases. Many polymers have been used as models of rigid rodlike polymer. The most commonly used polymer is poly(γ-benzyl α, l-glutamate) (PBLG) in a variety of solvents. Pioneering studies were carried out by Miller et al.[5–12] to obtain the phase boundaries for solutions of PBLG in dimethyl formamide using NMR and optical microscopy measurements. The experimentally observed phase diagram was qualitatively similar to that predicted by Flory for stiff chains. In addition, they observed gelation in the wide-biphasic phase contrary to the Flory theory that predicted isotropic and liquid crystalline phases coexisting. Miller et al.[9,13] also found that for gelation of PBLG in toluene there is a rapid increase of scattered intensity, while the scattering radius changes little. They believed the origin and nature of the gel phase to be a kinetic phenomenon and that the spinodal decomposition mechanism is dominant, leading to bicontinuous interconnected phases that have little possibility or driving force to rearrange further. The effect of side-chain flexibility on the phase equilibria has been included in Flory's theory by Wee and Miller,[7] and, later, Flory and his co-workers[14–

* To whom correspondence should be addressed.

Journal of Applied Polymer Science, Vol. 44, 2115–2125 (1992)
 CCC 0021-8995/92/122115-11$04.00

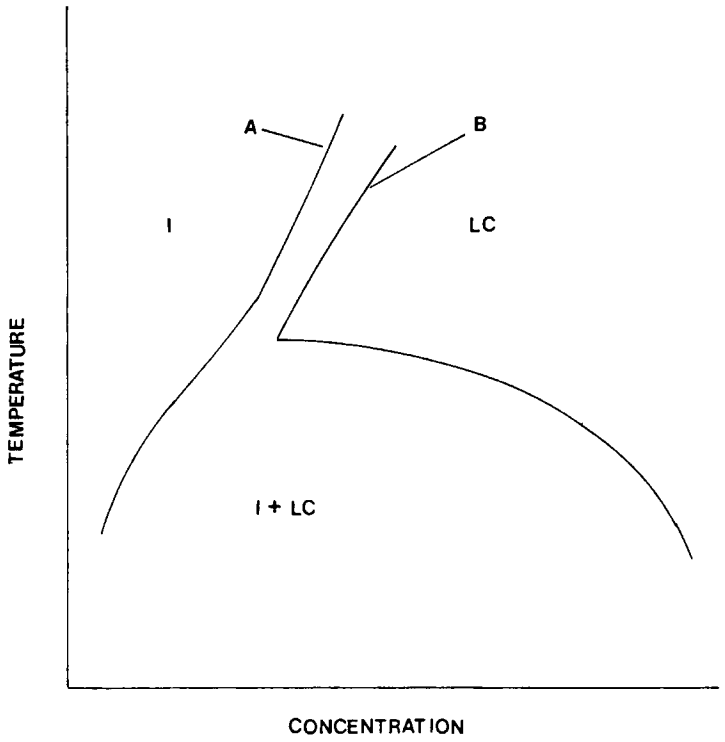

Figure 1 Schematic phase diagram for a rigid rod polymer solution (not drawn to scale) indicating all three phases: isotropic (I), liquid crystalline (LC), and biphase (I + LC). A and B are the concentrations corresponding to Robinson A and B points, respectively.

[16] incorporated polydispersity in their theoretical model to study its effect on phase equilibria. Experiments done by Sasaki et al.[17,18] and the recent rheological measurements made in our laboratories[19,20] also show that gelation occurs in the wide biphasic region at lower temperatures (Fig. 2). It is remarkable that a very dilute solution is able to exhibit gel behavior when the temperature is reduced by a few degrees. The process is also reversible, i.e., the solution is recovered on heating and the network is reformed on cooling. The nature of the boundary between the isotropic and gel phases at lower polymer concentrations is one of the issues investigated in this paper.

The diffusion of polymer chains in the isotropic phase has attracted many theoretical treatments. The translational diffusion coefficient D^0 and the rotational diffusion coefficient Θ^0 of a rodlike polymer in an infinitely dilute solution were calculated by Kirkwood and Riseman[21] to be

$$D^0 = \left(\frac{k_b T}{3\pi\eta_0 L}\right)\ln(L/d)$$

$$\Theta^0 = \left(\frac{3k_b T}{\pi\eta_0 L^3}\right)\ln(L/d) \qquad (1)$$

where L is the contour length of the rod, d is the diameter of the rod, and η_0 is the viscosity of the solvent. The Kirkwood–Riseman theory was generalized by Ullman, and by Hearst and Stockmayer, for stiff chains by adopting the various familiar models of a stiff chain. The reader should refer to Ref. 22 for a review of theoretical calculations of D^0 for stiff chains. The net qualitative result is that the radius of gyration R_g of the chain decreases as the degree of chain stiffness decreases and, consequently, D^0 increases since $D^0 \sim R_g^{-1}$ for infinitely dilute solutions.

As the concentration is increased, the polymers begin to interact with each other both thermodynamically and dynamically. The dynamical interactions consist of the screening of the hydrodynamic interactions and entanglement effects. These interactions are dominant if the polymer number concentration C_N is greater than or equal to L^{-3}. In general, at nonzero concentrations, two translational diffusion coefficients, viz. self, D_s, and mutual, D_m, are to be recognized. Of course, in the infinite dilution limit, $D_s = D_m = D^0$. In the semidilute region, where $L^{-3} \leq C_N \leq (dL^2)^{-1}$, the self-diffusion coefficient has been calculated by Doi and Edwards[23–25] using reptation ideas to be $D_s = D^0/2$. Also, the self-rotational diffusion coefficient has been predicted to

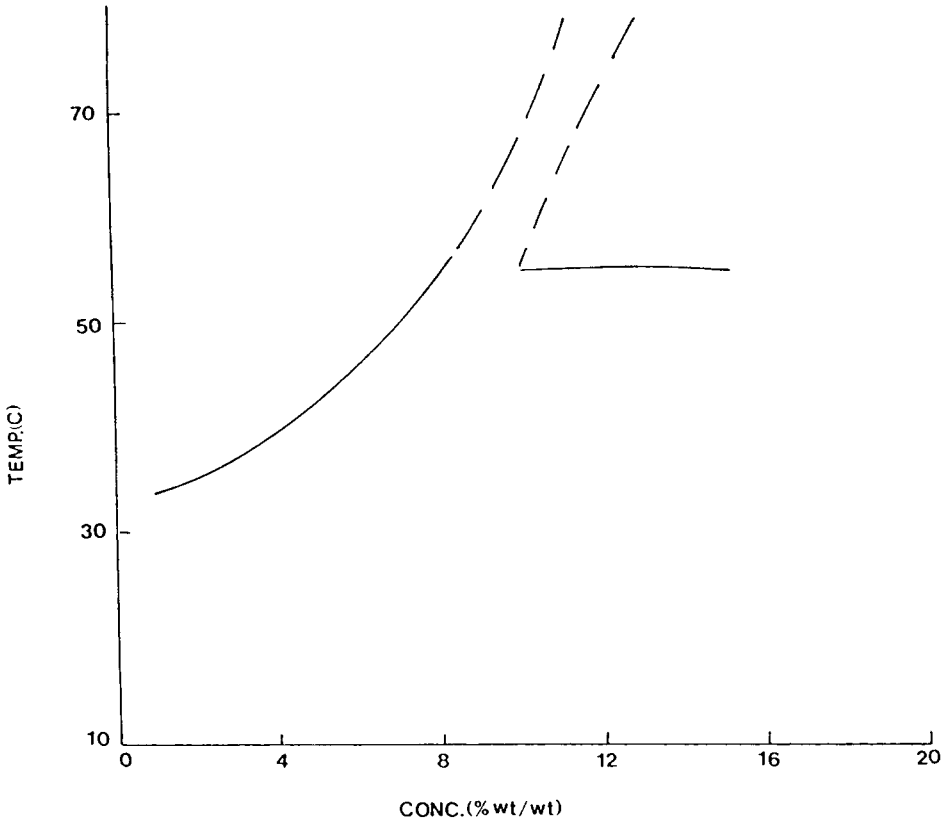

Figure 2 The phase diagram for the PBLG–BA system obtained from rheological measurements.

be proportional to $\langle C_N \rangle^{-2} L^{-9}$. The effect of partial chain stiffness on the transport coefficients in semidilute solutions continues to be a theoretical problem. Nevertheless, the limiting situation is the completely flexible chain where the scaling results

$$D_{\tilde{s}} L^{-2} C^{-7/4}$$
$$D_{\tilde{m}} L^{-2} C^{3/4} \qquad (2)$$

are well known. C is the polymer concentration.

Dynamic light scattering has proven to be a useful tool for the measurement of diffusion properties of polymers in solution. Such measurements offer an opportunity to verify the various theoretical predictions. There has been some recent work with the PBLG–dimethyl formamide system in semidilute solutions[26–29] and on the PBLG–1,2 dichloroethane system by Zero and Pecora.[30] In 1969, Ford et al.[31] studied the dynamic properties of PBLG using laser light scattering and they showed that the helix–coil transition of PBLG in dichloroacetic acid could be traced in terms of translational diffusional coefficients. Zero and Pecora[30] used conventional and depolarized light-scattering techniques to study the PBLG–1,2 dichloroethane system and made many findings. The mutual diffusion coefficient in semidilute solutions was found to be roughly two-thirds of the infinite-dilution value and had little concentration dependence. The rotational diffusion coefficient in semidilute solutions was found to be proportional to $C^{-2} L^{-8}$. Russo et al.[26] showed that the mutual translational diffusion coefficient increases with concentration for the PBLG–DMF system, and they attributed it to a repulsive thermodynamic contribution. Above the overlap concentration, a slow decay mode was found, suggesting delayed onset of entanglement. The measurement of D and Θ using the dynamic light-scattering technique for PBLG in benzyl alcohol is the primary objective of the present study.

In the gel phase formed by the stiff chains such as PBLG, the junction points are not permanent cross-links, but are generally believed to be formed by physical entanglements.[5] These physical cross-links make the gels thermoreversible, with the gels going into solution on heating and reforming the network upon cooling. More basic than determining the phase boundaries are the questions concerning the definition and identification of the gel phase and the molecular origins of such a phase. It is of interest

to understand the onset, the equilibrium, and the dynamic properties of this gel phase. These questions pose considerable difficulties to the successful development of a new theory that can describe the dynamics of such polymers in all phases. We have attempted to make a systematic study for each phase for the PBLG–benzyl alcohol (BA) system. Experiments, as well as the theory and simulations, are being carried out to get a better understanding of the gelation process. In a previous publication, we had determined the phase boundaries of the PBLG–BA system using rheological measurements,[20] and had studied the rheological properties of the system. We have also studied the supramolecular structure of the PBLG–BA system using static light scattering.[32]

Prins and co-workers[33,34] and Tanaka et al.[35] have shown that the autocorrelation function of scattered intensity can be related to the elastic properties of the gel network. In cross-linked polyacrylamide gels, Tanaka et al.[35] showed that the autocorrelation function of the scattered intensity can be fitted to a single exponential. The decay constant depends on the shear modulus and friction factor of the gel. The decay rate is given by $\Gamma = (Gq^2)/f$, where f is the frictional force per unit volume on the fiber network as it moves with unit velocity with respect to the gel liquid, G is the shear modulus for transverse displacements of the fiber network, and q is the scattering vector.

The technique of dynamic light scattering has been applied to both permanently cross-linked and entangled networks. Experiments by Munch et al.[36] on both types of systems indicate that the measured diffusion coefficient for cross-linked polymer networks and for semidilute solutions show the same increase in effective diffusion coefficient D_z with concentration $D_z \sim C^{0.7}$, which compares well with the scaling prediction $D_z \sim C^{0.75}$. Whereas in the early literature only "single exponential" behavior was reported, complex relaxation behavior is normally observed for semidilute solutions and gels, and an additional slow mode, which increases in amplitude as the concentration increases, is often detected in the time correlation function.

In this paper, we report the concentration and temperature dependencies of the diffusion coefficients obtained from dynamic light-scattering studies for the PBLG–BA system. These studies were made at low polymer concentrations, both in the isotropic and gel phases. To understand the aggregation behavior, the total intensity has been measured as a function of temperature at different concentrations. Also, we have monitored the scattered intensity as a function of time after the sample is subjected to a temperature quench into the gel phase. The persistence length of the chain has been estimated from the dilute solution data. The concentration dependence of the self-translational diffusion coefficient is also obtained by using Flory's theoretical expression for the osmotic compressibility.

EXPERIMENTAL

PBLG purchased from Sigma Chemicals (M.W. = 318,000, catalog no. P-5136, lot no. 96F-5103) was treated to reduce the dust by dissolving in DMF and filtering into a large excess of vigorously stirred, twice distilled, twice-filtered water via a 0.2 μm Teflon filter (Millipore FG type) to precipitate the PBLG. This sample was vacuum-dried at room temperature. The resultant polymer was dissolved in dioxane and filtered into water as above using the same type of filter. The sample was dried and dissolved in DMF and, finally, precipitated out by addition of methanol. The precipitate was then vacuum-dried at room temperature and redissolved in benzyl alcohol at 70°C to make solutions, with the concentrations being expressed as weight percent. Benzyl alcohol used as solvent was purchased from Aldrich Chemical Co. (catalog no. 10800-6, lot. no. 0229KL).

Light-scattering measurements were made within about 8 h of dissolving the polymer. We did not see any signs of degradation after the measurements. The sample cells were exhaustively rinsed in twice-filtered, twice-distilled, dust-free water and heat-dried before introduction of the polymer solutions. It was not possible to filter the polymer solutions into the sample cells because of very high viscosity ($[\eta] = 494.5$ mL/g) and gel formation at room temperatures.

The dynamic light-scattering studies were performed in the laboratory using a spectrometer previously described.[26] An argon-ion laser (Spectra Physics model 165) provided a beam of light at 514.5 nm wavelength. Correlation functions were generated by a digital correlator (Langley Ford Instruments models CM-64 and CM-1096). Samples were visually inspected for the presence of dust using a microscope, which views the actual scattering volume seen by the photomultiplier detector. The normalized field autocorrelation function $g^{(1)}(\tau)$, for each sample at a given condition was obtained from the point-by-point summation of correlation functions from the acceptable runs out of 12 attempts. Each run was of 20 min duration and the same cri-

teria as described in Ref. 26 were used to determine the acceptability.

The observed $g^{(1)}(\tau)$ are not single exponentials. We have assumed in this paper that $g^{(1)}(\tau)$ are not single exponentials. We have also assumed in this paper that $g^{(1)}(\tau)$ is a sum of two exponentials:

$$g^{(1)}(\tau) = A_1\exp(-T_1\tau) + A_2\exp(-T_2\tau) \quad (3)$$

The decay rates T_1 and T_2 are obtained using the multiexponential fit algorithm described in Ref. 26. Assuming rigid body motion for the polymer in dilute solutions, the decay rates are expressed in terms of translational and rotational diffusion coefficients D and Θ as

$$T_1 = q^2D, \text{ and,}$$
$$T_2 = T_1 + 6\Theta \quad (4)$$

where q is the scattering vector, $q = [(4\pi n)/\lambda]\sin(\theta_s/2)$, where n is the sample refractive index; λ, the vacuum wavelength of the incident laser beam; and θ_s, the scattering angle. Of course, the separation of the translational and rotational motion assumed here is strictly valid only in dilute solutions. Nevertheless, we have determined D and Θ for all experimental conditions studied here, based on fitting the experimental $g^{(1)}(\tau)$ to a double exponential. Concentration dependence of the self-translational diffusion coefficient is obtained by using Flory's theoretical expression for the osmotic compressibility.[2]

RESULTS AND DISCUSSION

Consider a PBLG-BA solution with the polymer concentration of 1%. The experimentally measured normalized field autocorrelation function, $g^{(1)}(\tau)$, is presented in Figures 3(a)-(c), as a function of time for different temperatures. At high temperatures, such as 70°C [Fig. 3(a)], $g^{(1)}(\tau)$ is decaying monotonically with time. $g^{(1)}(\tau)$ could not be fitted to a single exponential and the procedures described in the preceding section were followed to obtain the transport coefficients. As the temperature is lowered toward the gel point ($\simeq 32$°C), the correlation function exhibits a damped oscillatory decay, as shown in Figure 3(b). This pattern appears suddenly with a decrease in temperature of about 1°C, and we take the gelation temperature to be the temperature at which the oscillatory behavior sets in. The damped

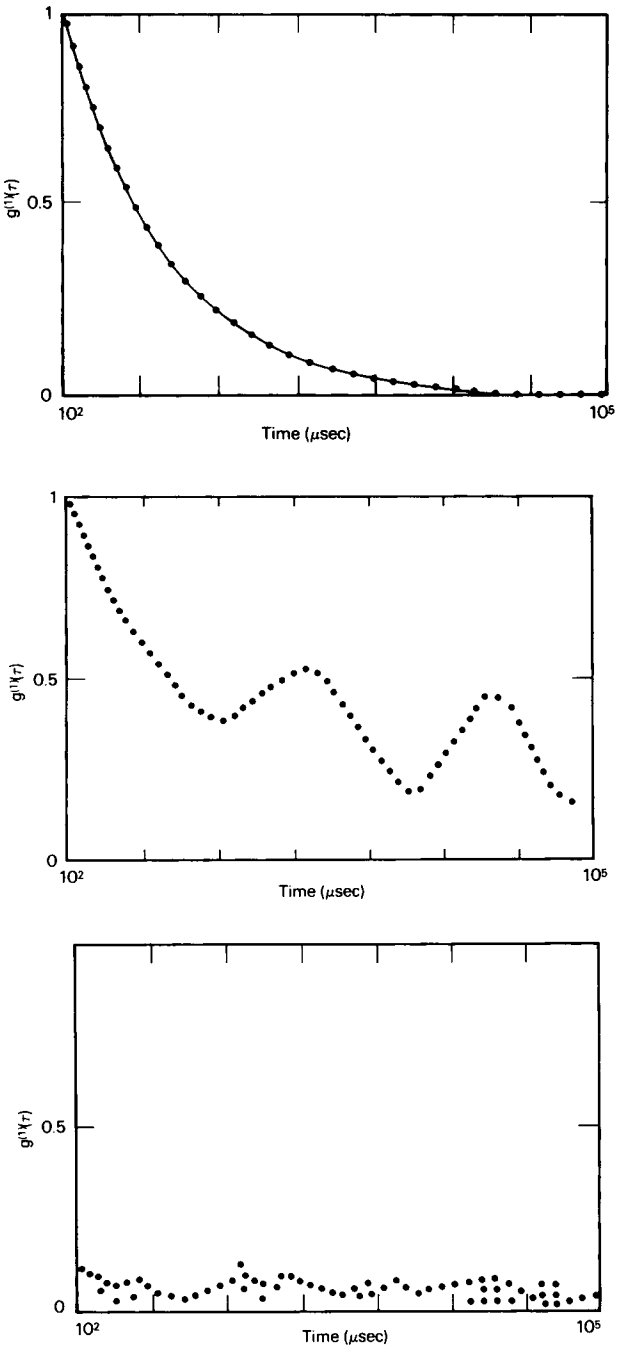

Figure 3 (a) A typical normalized base-line substrated correlation function at low concentrations and above gel temperatures (concentration = 1%, T = 70°C). (b) Typical correlation function at the gel temperature (concentration = 1%, $T \simeq 32$°C). (c) Typical correlation function well below the gel temperature (concentration = 1%, $T \simeq 25$°C).

oscillatory decay may be due to a nonequilibrium mass flow during gelation, with the polymer and solvent making in opposite directions. At temperatures

below the gelation temperature ($\simeq$ 25°C), the correlation function is essentially independent of time, as shown in Figure 3(c). The damped oscillatory decay of Figure 3(b) actually persists only for about 3 h and essentially settles into the pattern of Figure 3(c) while the temperature is maintained constant, indicating the kinetic nature of the formation of the gel phase. The decay pattern of Figure 4(c) for temperatures near the gel phase is quite like that reported already by Pines and Prins[33] for other aggregating systems.

Accompanying the change in the nature of $g^{(1)}(\tau)$ as the temperature is lowered, there is also a tremendous change in the scattered intensity. On entering the gel phase, the scattered intensity appears to diverge. The temperature at which this happens depends on the polymer concentration. The temperature dependence of the scattered intensity at various polymer concentrations is given in Figure 4. In an attempt to understand the nature of the gelation process, we have monitored the time dependence of the scattered intensity after temperature quench. A 5% concentration sample is quenched from 70 to 25°C within 2 s, and the time evolution of the scattered intensity is shown in Figure 5. The observed growth in intensity with time is indicative of aggregation process and is not consistent with the mechanism of spinodal decomposition.[33,34] In fact, the data of Figure 5 for times greater than t_0 can be fitted to an empirical Avrami equation with the Avrami exponent of $\sim$ 1.5, indicating the presence of diffusion-controlled fibrillar formation as the mechanism of gelation.

As pointed out earlier, the correlation function $g^{(1)}(\tau)$ in the isotropic phase is fitted to a double exponential and the translational and rotational diffusion coefficients are obtained using eqs. (3) and (4). For example, the decay rates T_1 and T_2 of 1% concentration solution at 70°C are plotted against the square of the scattering vector in Figure 6. Both T_1 and T_2 are linear in q^2 in accordance with eq. (4). D and Θ are obtained from the slopes and intercept of T_1 and T_2, respectively. For the higher concentration samples (about 1% and higher), at low angles (< 60°), the amplitude of the second decay rate T_2 is only about 5–10% of the total amplitude, while at higher angles (> 60°), the amplitude of T_2 is about 20–25% of the total amplitude. For the lower concentration samples, the relative amplitudes of T_2 are much smaller, though observable, indicating effects of polydispersity, other diffusion and bending effects, aggregation, coupling between different diffusion modes, etc.

The temperature dependence of the translational diffusion coefficient D obtained as above for 1%

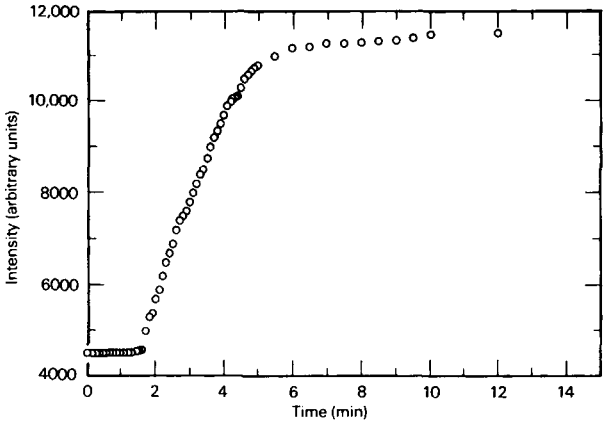

Figure 5 Plot of intensity vs. time at 35°C, for a 5% concentrated sample quenched from 70 to 25°C.

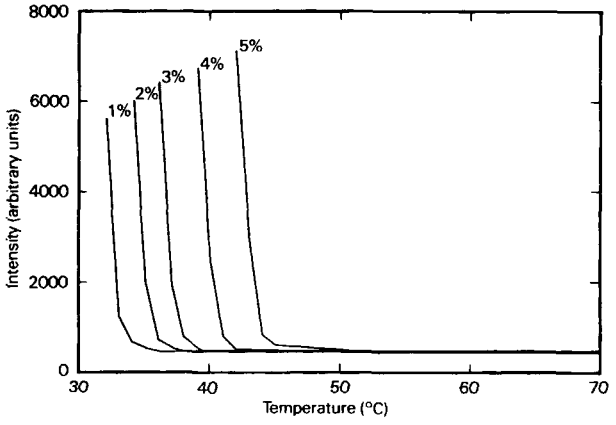

Figure 4 Plot of intensity vs. temperature for different concentration PBLG–BA solutions (θ = 90°).

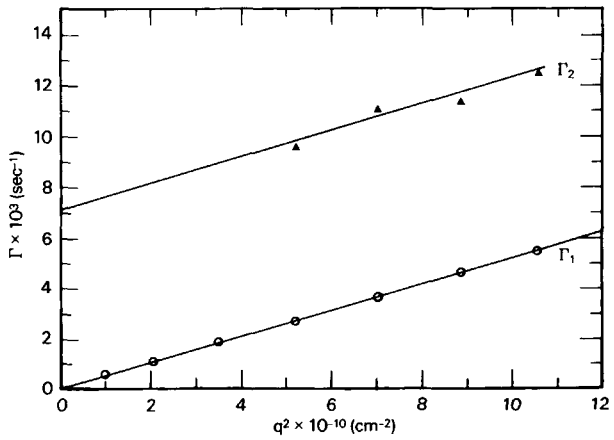

Figure 6 Plot of T_1 and T_2 vs. q^2 (angular dependence of D and Θ for 1% concentration solution at 70°C).

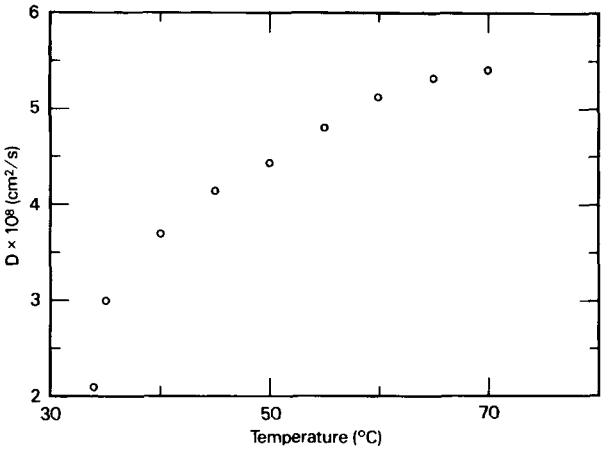

Figure 7 Plot of translational diffusion coefficient vs. temperature for 1% concentration of PBLG–BA solution, at $\theta = 90°$.

concentration solution in the isotropic phase is given in Figure 7. Although D cannot be obtained in the gelation temperature due to the oscillatory nature of $g^{(1)}(\tau)$, D is finite and measurable at temperatures even 1 degree above the gelation temperature. The decrease in D is more rapid as the temperature is lowered further. This may be because of some conformational changes of the polymer chain as the temperature is reduced, causing formation of bundles of three or four chains, which, upon reaching the gelation temperatures, aggregate to form an interconnected microfibrillar network.

We now proceed to discuss the concentration dependence of D and Θ at different temperatures. As pointed out in the Introduction, there are two concentration regimes, namely, dilute and semidilute, separated by the overlap concentration c^*. The overlap concentration[37] is given approximately by

$$c^* \sim \left(\frac{M}{N_A}\right)\left(\frac{4\pi R_g^3}{3}\right)^{-1}, \qquad (5)$$

where N_A is the Avogadro's number and R_g is the radius of gyration of the chain. We now estimate R_g using our earlier data on the intrinsic viscosity $[\eta]$ of PBLG–BA solutions[20] and the Einstein formula. We found that

$$[\eta] = KM_{\text{eff}}^{3\nu-1}, \qquad (6)$$

where $\nu_{\text{eff}} = 0.82 \pm 0.01$ and

$$K = 4.3 \times 10^{-6}\ \text{mL/g} \qquad (7)$$

Taking $[\eta]$ to be related to R_g by the Einstein formula:

$$[\eta] = \frac{(\eta - \eta_0)}{\eta_0 c} = (5/2)(1/c)\left(\frac{4N\pi R_g^3}{3V}\right)$$

$$= (10/3)\left(\frac{\pi R_g^3 N_A}{M}\right) \qquad (8)$$

where η and η_0 are the viscosities of the solution and solvent, respectively, we estimate the radius of gyration in infinite dilute solution from eqs. (6), (7), and (8) as $R_g \sim 292$ Å.

Because of the Einstein assumption, we are probably underestimating the real value of R_g. Anyway, the use of this value of R_g in eq. (5) gives c^* to be 0.005 gm/cm^3 (0.5%).

For very dilute concentrations, up to 0.4% concentration, as shown in Figure 8, a plot of the translational diffusion coefficient vs. concentration is linear. On extrapolation to zero concentration, we obtain a linear concentration expansion for D:

$$D = D^0(1 + k_d c + \cdots) \qquad (9)$$

where the diffusion coefficient at infinite dilution, D^0, is given by $D^0 = 4.763 \times 10^{-8}$ cm^2/s and the coefficient k_d of the leading concentration term is given by $k_d = 3.384 \times 10^{-8}$ cm^3/g. Just for comparison purposes, D^0 is also consistent with the value estimated from the Stokes–Einstein relation (assuming a hard sphere of radius R_g):

$$D_{SE}^0 = \frac{k_b T}{6\pi\eta_0 R_g} = 4.59 \times 10^{-8}\ \text{cm}^2/\text{s} \qquad (10)$$

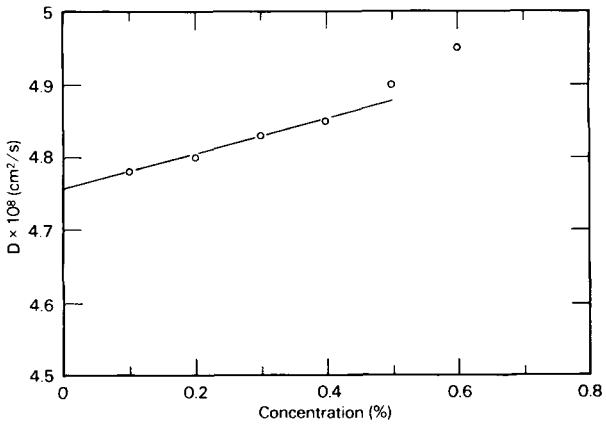

Figure 8 Plot of translational diffusion coefficient vs. concentration at 70°C in dilute solution regime.

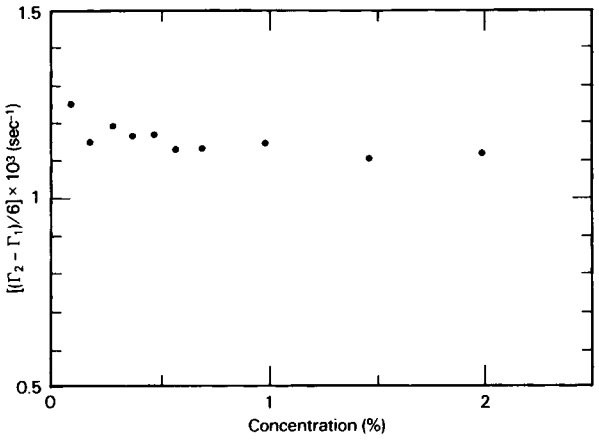

Figure 9 Plot of the rotational diffusion coefficient vs. concentration for PBLG-BA at 70°C.

where η_0 of benzyl alcohol at 70° is 2.4 centipoises and the above value of R_g is used.

Figure 9 is a plot of the rotational diffusion coefficient $\Theta = (T_2 - T_1)/6$ vs. concentration at 70°. No concentration dependence of the rotational diffusion coefficient is observed. On extrapolating the curve to zero concentration (getting an average value), we get a value for the rotational diffusion coefficient at infinite dilution to be about 1150 s^{-1}.

We now attempt to fit the experimental data to a model of a stiff chain. For the wormlike chain model of Kratky and Porod,[38] the radius of gyration is given by

$$R_g^2 = \frac{L}{6\lambda} - \frac{\lambda^2}{4} + \frac{\lambda^3 L}{4} - \lambda^4 L^2 \frac{[1 - \exp(-2\lambda L)]}{8} \quad (11)$$

where L is the contour length of the polymer chain and $(2\lambda)^{-1}$ is the presistence length Q. The dimensionless parameter $x = 2\lambda L$ for our PBLG-BA system is found to be 2.45 by fixing the effective exponent of the molecular weight dependence of $R_g^2 L^2$ to be -0.36 so as to be consistent with the radius of gyration exponent given in eq. (7). Knowing the value of x, the other parameter L is fitted from the amplitude of R_g given by eq. (11) to be 1248°.

Next, we use the generalization of the Kirkwood–Riseman theory of dynamics of flexible chains in infinitely dilute solutions to wormlike chains. By incorporating the effect of chain stiffness as a renormalized Kuhn length just as in the case of excluded volume effect,[39] $[\eta]$, D, and Θ are given by[40]

$$[\eta]_{KR} = \frac{N_A L}{6\eta_0 M\pi^2 \left(\sum \frac{l_1(\mu)}{2^{1/2}\mu^{3/2}h}\right)} \quad (12a)$$

$$\simeq N_A L^{3/2} \zeta(3/2)(6\pi)^{-1/2} \times \left[1/\lambda - \frac{1}{2L\lambda^2}(1 - e^{-2\lambda L})\right]^{1.5} \quad (12b)$$

$$D^0_{KR} = \left(\frac{8 \times 2^{1/2}}{3}\right) k_b T h \quad (13a)$$

$$\simeq \frac{[(4 \times 2^{1/2})}{(3\pi^{3/2})} \left(\frac{k_b T}{\eta_0}\right) \times \left[L/\lambda - \frac{1}{2\lambda^2}(1 - e^{-2\lambda L})\right]^{-1/2} \quad (13b)$$

and

$$\Theta^0_{KR} = \frac{3\pi^2 k_b T}{2L\left(\sum \frac{l_1(\mu)}{2^{1/2}\mu^{3/2}h}\right)} \quad (14a)$$

$$\simeq \left(\frac{3\pi}{8}\right)^{1/2} \left[\frac{k_b T}{\eta_0 \zeta(3/2)}\right] \times \left[L/\lambda - \frac{1}{2\lambda^2}(1 - e^{-2\lambda L})\right]^{-1.5} \quad (14b)$$

where

$$h = \frac{1}{\eta_0 [12\pi^3 L l_1(\mu)]^{1/2}} \quad (15)$$

and $l_1(\mu)$ is the mode-dependent step-length accounting for the chain stiffness. In obtaining eqs. (12b), (13b), and (14b) from eqs. (12a), (13a), and (14a), we have approximated $l_1(\mu)$ to be given by only the lowest mode, viz.

$$l_i(\mu) = \left[1/\lambda - \frac{1}{2L\lambda^2}(1 - e^{-2\lambda L})\right] \quad (16)$$

$\zeta(3/2)$ in these equations is the Riemann zeta function with the value of 2.612.

Now keeping L = 1248 Å and x = 2.45 (i.e., Q = 509 Å, $\lambda = 9.82 \times 10^{-30}$ A^{-1}), we obtain from eqs. (12b), (13b), and (14b), $[\eta]_{KR}$ = 814 mL/g,

$$D^0_{KR} = 4.29 \times 10^{-8} \frac{cm^2}{s},$$

$$\Theta^0_{KR} = 1145\ s^{-1}$$

Although the theoretical values from the generalized Kirkwood–Riseman theory for D^0 and Θ^0 are in remarkable agreement with the experimental data, the $[\eta]$ is only qualitatively correct.

It would be of considerable interest to measure R_g directly from light-scattering experiments. However, we found it very difficult to get this information, because of the highly nonlinear nature of the Zimm plot and significant intensity fluctuations at small wave vectors in the sample.

Figure 10 is a plot of D obtained experimentally vs. concentration extending into the semidilute region. We observe that on increasing concentration, at 70°C, the mutual translational diffusion coefficient increases.

For semidilute solutions of polymer chains, the scaling theory[41] predicts that

$$D \sim \xi^{-1} \sim c^{\nu_{\text{eff}}/(3\nu_{\text{eff}}-1)} \tag{17}$$

where ξ is the correlation length. Since ν_{eff} for PBLG in BA is 0.82, we expect D to be proportional to $c^{0.56}$ in the semidilute region. However, we find the effective power law, $D \simeq c^{0.2}$ (Fig. 11). This deviation implies that there is an additional variable arising from orientational interactions in addition to the overlap concentration that determines the diffusion coefficients.

The mutual diffusion coefficient is related to the self-diffusion coefficient D_s by

$$D_m = (M/N_A)(1-\nu_2)\left(\frac{\delta\pi}{\delta c}\right)\left(\frac{D_s}{k_bT}\right) \tag{18}$$

where $[(\delta\pi)/(\delta c)]$ is the osmotic compressibility

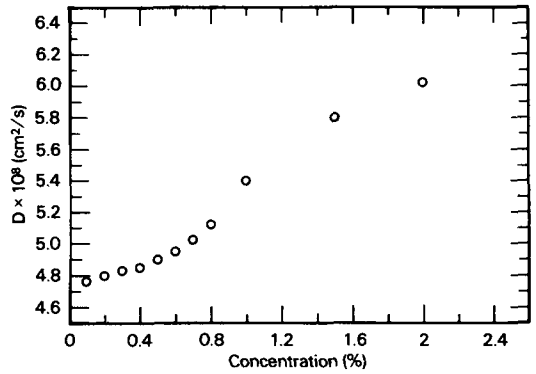

Figure 10 Plot of translational diffusion coefficient vs. concentration at 70°C for solutions extending into the semidilute regime.

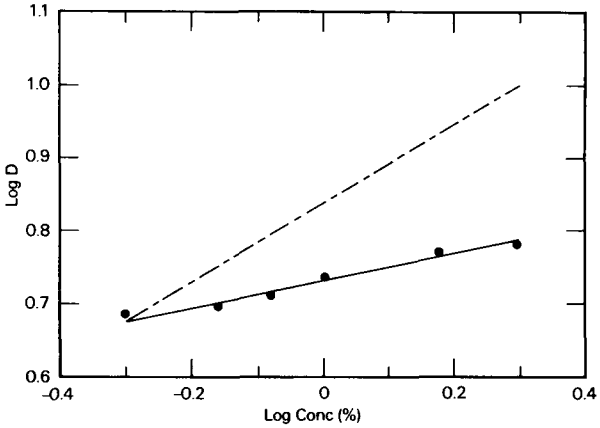

Figure 11 Plot of self-diffusion coefficient D_s vs. concentration.

and represents a driving force for diffusion due to concentration fluctuation, N^A is the Avogadro's number, and ν_2 is the specific volume of polymer of molecular weight M.

In the isotropic phase, $[(\delta\pi)/(\delta c)]$ is given by Flory's theory of stiff chains as

$$\left(\frac{\delta\pi}{\delta c}\right) = \left(\frac{-RT}{V_1}\left\{\frac{-1}{(1-c)} + \left(1-\frac{1}{y}\right) + 2\chi c\right\}\right. \tag{19}$$

where R is the gas constant, V_1 is the partial molar volume of the solvent, y is the axial ratio, and χ is the usual Flory–Huggin's interaction parameter. By comparing the theoretical phase diagram of Flory's theory and the experimental phase diagram of Figure 2, we have obtained an empirical temperature dependence of χ and the value of the axial ratio y as

$$\chi = -1.304 + \frac{440.6}{T}$$

$$y = 150$$

Taking M = 318,000, ν_2 = 0.769 cm^3/(gm − mol), D_s at 70° is calculated for different concentrations. The result is given in Figure 12. D_s is seen to be a decreasing function of concentration. Based on the scaling theory,

$$D_s \simeq c^{1-2\nu_{\text{eff}}/3\nu_{\text{eff}}-1} \tag{20}$$

we expect the exponent to be −0.81. We observe an apparent exponent of −0.75. Although the use of the Flory's expression is very approximate and may

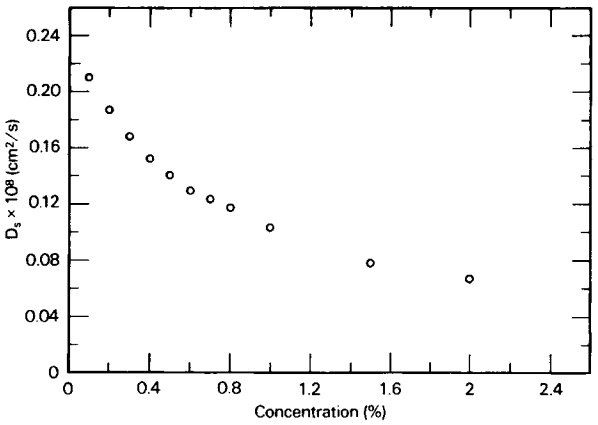

Figure 12 Log–Log plot of D vs. concentration in the semidilute regime. Experimental data $D \simeq c^{0.2}$ (solid line). Scaling prediction, $D \simeq c^{0.56}$ (dashed line).

be partly responsible for the discrepancy, the disagreement may be due to the coupling between the translational and rotational motions. It must also be pointed out that D_s is smaller than even the predicted limit[24,25] for rodlike chains, viz. $D^0/2$.

In addition, Θ is found to be independent of c in the semidilute solutions, in contrast to the Doi–Edwards prediction of $\Theta_s \simeq c^{-2}$ for rodlike polymers. Attempts to measure Θ by depolarized dynamic light scattering were not particularly successful because of the weak excess depolarized scattering from PBLG above that of the benzyl alcohol.

CONCLUSIONS

Dynamic light-scattering studies have been made at low polymer concentrations, both in the isotropic and gel phases, to study the concentration and temperature dependencies of the diffusion coefficients for the PBLG–BA system. For PBLG solutions above the gel temperature, and at low concentrations, the correlation functions are fit by double exponential decays. To understand the aggregation behavior, the total intensity has been measured as a function of temperature at different concentrations. The intensity appears to diverge at the gel point. Also, we have monitored the scattered intensity as a function of time after the sample is subjected to a temperature quench into the gel phase. The observed growth in intensity with time is indicative of aggregation process and indicates the diffusion-controlled fibrillar formation as the mechanism of aggregation. On decreasing temperature from 70°C and up to going into the gel phase, we observe a decrease in the translational diffusion coefficient, with the decrease more rapid as the temperature is lowered. On increasing concentration, in the dilute and semidilute concentration regimes we observe an increase in the mutual translational diffusion coefficient. The persistence length of the chain has been estimated from dilute solution data to be about 509 Å. We expect $D_m \simeq c^{0.56}$ in the semidilute region. However, we find the effective power law, $D_m \simeq c^{0.2}$, with the deviation implying that there is an additional variable arising from orientational interactions. The concentration dependence of the self-translational diffusion coefficient is obtained by using Flory's theoretical expression for the osmotic compressibility. We expect $D_s \simeq c^{0.44}$. We observe an apparent expression of -0.75. Although the use of Flory's expression is very approximate and may be partly responsible for the discrepancy, the disagreement may be due to coupling between the translational and rotational motions. The rotational diffusion coefficient has been measured and is found to be independent of concentration. At temperatures near the gel temperature, the normalized field autocorrelation function has an oscillating decay. At lower temperatures, in the gel phase, the correlation function is independent of time, and the diffusion coefficient cannot be measured using this technique.

Acknowledgment is made to the Center of UMass-Industry Research in Polymers, the National Science Foundation, and the Materials Research Laboratory at the University of Massachusetts.

REFERENCES

1. L. Onsager, *Ann. N.Y. Acad. Sci.*, **51,** 627 (1949).
2. P. J. Flory, *Proc. R. Soc. Lond. Ser. A.*, **234,** 60 (1956).
3. C. Robinson, *Trans. Faraday Soc.*, **52,** 571 (1955).
4. C. Robinson, *Tetrahedron,* **13,** 219 (1961).
5. W. G. Miller, L. L. Wu, E. L. Wee, G. L. Santee, J. H. Rai, and K. D. Goeber, *Pure Appl. Chem.*, **38,** 37 (1974).
6. W. G. Miller, *Annu. Rev. Phys. Chem.*, **29,** 519 (1980).
7. E. L. Wee and W. G. Miller, *J. Phys. Chem.*, **79,** 1446 (1971).
8. W. G. Miller, J. H. Rai, and E. L. Wee, *Liquid Crystals and Ordered Fluids,* J. F. Johnson and R. S. Porter, Eds., Plenum Press, New York, 1974, p. 243.
9. W. G. Miller, L. Kou, K. Tohyama, and V. Voltaggio, *J. Polym. Sci. Polym. Symp.*, **65,** 91 (1978).
10. K. Tohyama and W. G. Miller, *Nature,* **289,** 813 (1981).
11. P. R. Russo and W. G. Miller, *Macromolecules,* **16,** 1690 (1983).
12. P. R. Russo and W. G. Miller, *Macromolecules,* **17,** 1324 (1984).
13. P. R. Russo, P. Magestro, M. Mustafa, M. J. Saunder,

and W. G. Miller, *Am. Chem. Soc. Polym. Prepr.*, **29,** (1986).
14. P. J. Flory and A. Abe, *Macromolecules,* **11,** 1119 (1978).
15. A. Abe and P. J. Flory, *Macromolecules,* **11,** 1122 (1978).
16. P. J. Flory and R. S. Frost, *Macromolecules,* **11,** 1126 (1978).
17. S. Sasaki, M. Hikata, C. Shiraki, and I. Uematsu, *Polym. J. (Tokyo),* **14,** 205 (1982).
18. S. Sasaki, K. Tokuma, and I. Uematsu, *Polym. Bull. (Berl.),* **10,** 539 (1983).
19. A. K. Murthy and M. Muthukumar, *Macromolecules,* **20,** 564 (1987).
20. P. Shukla and M. Muthukumar, *Polym. Eng. Sci.,* **28**(20), 1304 (1988).
21. J. G. Kirkwood and J. Riseman, *J. Chem. Phys.,* **18,** 87 (1982).
22. H. Yamakawa, *Modern Theory of Polymer Solutions,* Harper & Row, New York, 1971.
23. M. Doi, *J. Phys. (Paris),* **36,** 607 (1975).
24. M. Doi and S. F. Edwards, *J. Chem. Soc. Faraday Trans. 2,* **74,** 560 (1978).
25. M. Doi and S. F. Edwards, *J. Chem. Soc. Faraday Trans. 2,* **74,** 918 (1978).
26. P. R. Russo, F. E. Karasz, and K. H. Langley, *J. Chem. Phys.,* **80**(10), (1984).
27. K. Kubota and B. Chu, *Biopolymers,* **22,** 1461 (1983).
28. K. Kubota, Y. Tominaga, S. Fujime, *Macromolecules,* **19,** 1604 (1986).
29. K. Kubota, Y. Tominaga, S. Fujime, J. Otomo, and K. Ikegami, *Biophys. Chem.,* **23,** 15 (1985).
30. K. M. Zero and R. Pecora, *Macromolecules,* **15,** 87 (1982).
31. N. C. Ford, Jr., W. Lee, and F. E. Karasz, *J. Chem. Phys.,* **50,** 3098 (1969).
32. P. Shukla and M. Muthukumar, *J. Polym. Sci., Polym. Phys. Ed.,* **29,** 1373 (1991).
33. E. Pines and W. Prins, *Macromolecules,* **6,** 888 (1973).
34. K. L. Wun, G. T. Feke, and W. Prins, *Faraday Discuss. Chem. Soc.,* **57,** 146 (1974).
35. T. Tanaka, L. O. Hocker, and G. B. Benedek, *J. Chem. Phys.,* **59,** 5151 (1973).
36. J. P. Munch, S. J. Candau, J. Herz, and G. Hild, *J. Phys. (Paris),* **38,** 971 (1977).
37. P. G. de Gennes, *Scaling Concepts in Polymer Physics,* Cornell University Press, Ithaca, NY, 1979.
38. O. Kratky and G. Porod, *Rev. Trav. Chim.,* **68,** 1106 (1949).
39. M. Demeuse and M. Muthukumar, *Macromolecules,* **18,** 1173 (1985).
40. M. Muthukumar, to appear.
41. M. Doi and S. F. Edwards, *The Theory of Polymer Solutions,* Clarendon Press, Oxford, UK, 1986.

Received January 25, 1991
Accepted July 8, 1991